Ji-Eun Byun
Date: 24 May 2026

Transport network subjected to a mainshock-aftershock sequence

For illustration, we consider the Eastern Massachusetts (EMA) benchmark highway network, illustrated in Figure 1a. We assume that it is subjected to a seismic risk of mainshock and aftershock, where the risk is represented by an areal source. With the areal source with region $|P|$, the location of the mainshock's epicentre $\boldsymbol{l}_0 = \left(l_{0,x}, l_{0,y}\right)$ follows the distribution

$$f_{\boldsymbol{L}_0}(\boldsymbol{l}_0) = \begin{cases} \dfrac{1}{|P|} & \text{if } \left(l_{0,x}, l_{0,y}\right) \in P, \\ 0 & \text{otherwise.} \end{cases} \tag{1}$$

The mainshock's magnitude is assumed to follow the truncated exponential distribution [Cosentino et al., 1977, Lee et al., 2011] as

$$f_{M_0}(m_0) = \begin{cases} \dfrac{\beta \exp\left[-\beta(m_0 - m_{0,\min})\right]}{1 - \exp\left[-\beta(m_{0,\max} - m_{0,\min})\right]} & \text{for } m_{0,\min} \le m_0 \le m_{0,\max}, \\ 0 & \text{otherwise.} \end{cases} \tag{2}$$

where the parameter are set as $\beta = 0.76$, $m_{0,\min} = 6.0$, and $m_{0,\max} = 8.5$.

The number of aftershocks K following the mainshock is modelled using the modified Omori law [Utsu et al., 1995], which describes the temporal decay of aftershock activity through the instantaneous occurrence rate

$$\lambda(t) = \frac{K_0}{(t+c)^p}, \tag{3}$$

where t is the elapsed time since the mainshock, $c > 0$ is a small time offset, p controls the decay rate, and

$$K_0 = 10^{\,a+b(m_0 - m_{0,\min})} \tag{4}$$

is a productivity constant scaling with the mainshock magnitude m_0, so that larger mainshocks generate proportionally more aftershocks. We set $a = -1.67$, $b = 0.91$, $c = 0.05$ days, and $p = 1.08$ [Reasenberg and Jones, 1989]. Assuming aftershock occurrences follow a non-homogeneous Poisson process with rate $\lambda(t)$, the total number of aftershocks K within a time window $[0, T]$ is Poisson-distributed with mean

$$\Lambda(T) = \int_0^T \lambda(t)\,\mathrm{d}t = \frac{K_0}{1-p}\left[(T+c)^{1-p} - c^{1-p}\right], \tag{5}$$

leading to

$$f_{K|M_0}(k \mid m_0) = \frac{\Lambda(T)^k \exp[-\Lambda(T)]}{k!}, \quad k = 0, 1, \ldots, K_{\max}. \tag{6}$$

We set $T = 7$ days and $K_{\max} = 20$.

To simulate the locations aftershocks, let R_t and V_t denote the distance and direction from the mainshock's epicentre to the t-th aftershock's, respectively, for $t = 1, \ldots, K_{\max}$. The aftershock is assumed

equally likely to occur in any direction from the mainshock epicentre, with the distance following the radial decay [Felzer and Brodsky, 2006], i.e.

$$f_{R_t|K}(r_t \mid k) = \begin{cases} \dfrac{1-n}{r_{\max}^{1-n} - r_{\min}^{1-n}}\, r_t^{-n}, & t \le k \text{ and } r_t \in [r_{\min}, r_{\max}] \\ \delta(r_t), & t > k \\ 0, & \text{otherwise,} \end{cases} \tag{7}$$

where $n = 1.35$ and $\delta(\cdot)$ denotes the Dirac delta, so that $R_t = 0$ deterministically when $t > k$, and

$$f_{V_t|K}(v_t \mid k) = \begin{cases} \dfrac{1}{2\pi}, & t \le k \text{ and } v_t \in [0, 2\pi) \\ \delta(v_t), & t > k \\ 0, & \text{otherwise.} \end{cases} \tag{8}$$

Given $\boldsymbol{L}_0$, R_t, and V_t, the t-th aftershock location $\boldsymbol{L}_t$ is calculated as

$$\boldsymbol{L}_t = \boldsymbol{L}_0 + R_t\,(\cos V_t,\, \sin V_t), \tag{9}$$

i.e. $f_{\boldsymbol{L}_t|\boldsymbol{L}_0,R_t,V_t}(\boldsymbol{l}_t \mid \boldsymbol{l}_0, r_t, v_t) = \delta\big(\boldsymbol{l}_t - \boldsymbol{l}_0 - r_t(\cos v_t, \sin v_t)\big)$. The t-th aftershock's magnitude is assumed to follow the same truncated exponential distribution as the mainshock, conditioned on the mainshock's magnitude and the active-slot indicator. Following Båth's law [Båth, 1965], the upper bound is set to $m_0 - \Delta m$ with $\Delta m = 1.2$, i.e.

$$f_{M_t|M_0,K}(m_t \mid m_0, k) = \begin{cases} \dfrac{\beta\, \exp\left[-\beta(m_t - m_{t,\min})\right]}{1 - \exp\left[-\beta(m_0 - \Delta m - m_{t,\min})\right]} & \text{for } t \le k \text{ and } m_{t,\min} \le m_t \le m_0 - \Delta m, \\ \delta(m_t), & \text{for } t > k, \\ 0, & \text{otherwise,} \end{cases} \tag{10}$$

where $\beta = 0.76$ is inherited from the mainshock distribution and $m_{t,\min} = 4.5$ is set as the engineering threshold for damaging shaking.

The peak ground acceleration (PGA, in g) $A_{t,n}$ at edge n from shock t, $i = 0, 1, \cdots, K_{\max}$ is assumed to follow a lognormal distribution conditional on the magnitude M_t, i.e.

$$f_{A_{t,n}|M_t}(a_{t,n} \mid m_t) = \frac{1}{a_{t,n}\,\sigma_A\sqrt{2\pi}} \exp\left[-\frac{(\ln a_{t,n} - \mu_A(m_t, r_{t,n}))^2}{2\sigma_A^2}\right], \tag{11}$$

with log-mean $\mu_A(m_t, r_{t,n})$ given by the attenuation relationship [Campbell, 1997, Lee et al., 2011] as

$$\mu_A(m_t, r_{t,n}) = \ln 0.55 - 3.512 + 0.904\, m_t - 1.328\, \ln\sqrt{r_{t,n}^2 + [0.149\exp(0.647\, m_t)]^2}, \tag{12}$$

where $r_{t,n}$ is the distance between edge n's midpoint and the epicentre of event t, the $\ln 0.55$ term scales the horizontal peak ground acceleration to the pseudo-spectral acceleration.[1] The log-standard deviation $\sigma_A = 0.52$ represents the aleatory variability of the attenuation model [Campbell, 1997].

[1] The site-condition and fault-type terms have been omitted under the assumption of alluvium or firm soil and strike-slip faulting Lee et al. [2011].

For each edge $n = 1, \ldots, N$, let $D_{t,n}$ denote the Park–Ang damage indices of edge n after the mainshock and aftershock respectively. Following the demand model of Ghosh et al. [2015], $\ln D_{0,n}$ and $\ln D_{t,n}$ are conditionally Gaussian, i.e.

$$f_{D_{0,n}|A_{0,n}}(d_{0,n} \mid a_{0,n}) = \frac{1}{d_{0,n}\,\varepsilon_0\sqrt{2\pi}} \exp\left[-\frac{(\ln d_{0,n} - \mu_0(a_{0,n}))^2}{2\varepsilon_0^2}\right], \tag{13}$$

$$f_{D_{t,n}|A_{t,n},D_{t-1,n}}(d_{t,n} \mid a_{t,n}, d_{t-1,n}) = \frac{1}{d_{t,n}\,\varepsilon'\sqrt{2\pi}} \exp\left[-\frac{(\ln d_{t,n} - \mu_t(a_{t,n}, d_{t-1,n}))^2}{2\varepsilon_t^2}\right], \tag{14}$$

with conditional means

$$\mu_0(a_{0,n}) = \alpha_0 + \beta_0 \ln a_{0,n}, \tag{15}$$

$$\mu_t(a_{t,n}, x_{t-1,n}) = \alpha' + \beta' \ln a_{t,n} + \gamma' \ln x_{t-1,n} + \delta' \ln a_{t,n} \cdot \ln x_{t-1,n}, \tag{16}$$

where $(\alpha_0, \beta_0, \varepsilon_0) = (-1.91,\ 2.51,\ 0.70)$ are the single-shock parameters, and $(\alpha', \beta', \gamma', \delta', \varepsilon') = (-1.65,\ 0.71,\ 0.19,\ -0.33,\ 0.68)$ are the multi-shock average model parameters [Ghosh et al., 2015]. These parameters are assumed uniformly across all edges.[2] To enforce the monotonicity property $D_{t,n} \geq D_{t-1,n}$ implied by the cumulative nature of damage indices, the conditional distribution in (14) is truncated below at $d_{t-1,n}$ and renormalised.

The operational state $X_{i,n}$ of edge n, $n = 1, \ldots, N$, after shock i, $i = 0, 1$, is a deterministic function of the damage index $D_{i,n}$, given by

$$X_{i,n} = \begin{cases} 1, & d_{i,n} < 0.4 \\ 0, & d_{i,n} \geq 0.4, \end{cases} \qquad i = 0, 1, \quad n = 1, \ldots, N. \tag{17}$$

where the threshold $d_{i,n} = 0.4$ corresponds to the conventional boundary between moderate and severe damage, beyond which the bridge is considered closed to traffic [Ghosh et al., 2015].

The system state S_i after the i-th shock is defined as a deterministic function of the edge states $\boldsymbol{X}_i = (X_{i,1}, \ldots, X_{i,N})$ and the resulting network topology, taking the value

$$S_i = \begin{cases} 1, & \text{if at least 95\% of the population can reach a destination node in } \mathcal{V}_{\text{dest}} \\ & \text{taking no more than 15 minutes longer than the nominal (undamaged-network) travel time,} \\ 0, & \text{otherwise.} \end{cases} \tag{18}$$

The nodes and edges of the EMA highway benchmark network are summarised in Tables 1 and 2. We set $\mathcal{V}_{\text{dest}} = \{n_{22},\ n_{66}\}$.

[2] While there parameters were originally derived for a single-column box girder bridge in California, we adopt them for demonstration purposes.

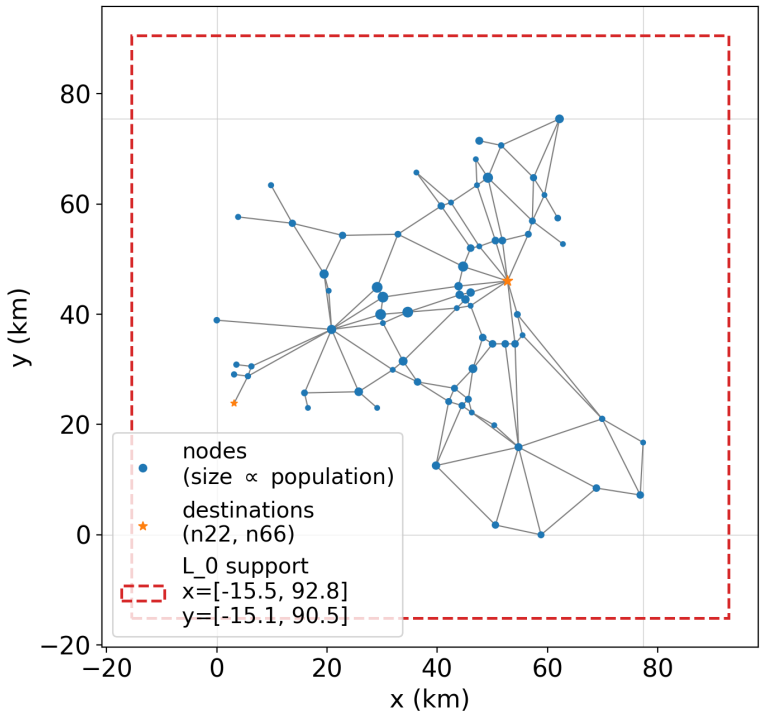

(a)

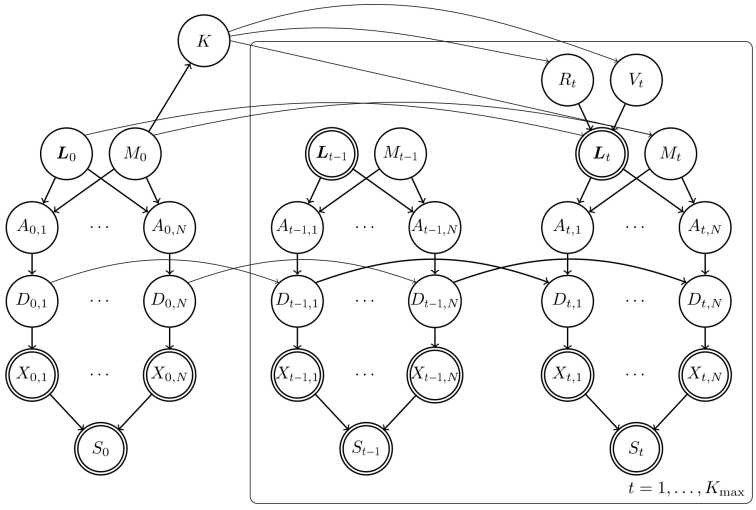

(b)

Figure 1. EMA benchmark highway network subjected to a mainshock–aftershock sequence. (a) network and (b) graphical representation of the probabilistic model. Random and deterministic variables are indicated respectively by single- and double-stroke circles.

Node	x (km)	y (km)	pop.	Node	x (km)	y (km)	pop.	Node	x (km)	y (km)	pop.
n_1	62.15	75.44	1767	n_{26}	45.10	42.69	1506	n_{51}	68.85	8.48	963
n_2	47.61	71.46	1193	n_{27}	43.53	41.12	0	n_{52}	58.80	0.00	600
n_3	51.58	70.63	274	n_{28}	46.04	41.54	0	n_{53}	50.54	1.78	869
n_4	46.98	68.12	0	n_{29}	54.51	39.97	539	n_{54}	39.76	12.56	1478
n_5	36.20	65.71	0	n_{30}	29.09	44.89	3428	n_{55}	9.84	63.41	137
n_6	49.18	64.77	2882	n_{31}	30.13	43.11	3428	n_{56}	3.87	57.65	137
n_7	57.44	64.77	725	n_{32}	29.72	39.97	3428	n_{57}	13.71	56.50	826
n_8	47.19	63.41	0	n_{33}	34.63	40.39	3428	n_{58}	22.81	54.30	828
n_9	59.43	61.63	0	n_{34}	30.13	38.40	0	n_{59}	19.46	47.29	2141
n_{10}	40.70	59.64	842	n_{35}	33.80	31.49	1880	n_{60}	20.82	37.25	2141
n_{11}	42.48	60.27	0	n_{36}	36.41	27.73	945	n_{61}	0.00	38.92	356
n_{12}	61.84	57.44	451	n_{37}	48.24	35.78	982	n_{62}	3.56	30.87	223
n_{13}	57.23	56.92	554	n_{38}	50.01	34.63	982	n_{63}	6.28	30.55	223
n_{14}	56.50	54.51	554	n_{39}	52.32	34.63	982	n_{64}	3.14	29.09	223
n_{15}	62.78	52.73	0	n_{40}	54.10	34.63	982	n_{65}	5.65	28.77	223
n_{16}	50.54	53.36	1012	n_{41}	55.46	36.20	0	n_{66}	3.14	23.86	223
n_{17}	51.79	53.36	1012	n_{42}	46.46	30.13	1855	n_{67}	15.90	25.74	504
n_{18}	46.04	52.00	1012	n_{43}	43.11	26.58	619	n_{68}	16.53	23.02	0
n_{19}	47.61	52.32	0	n_{44}	42.06	24.17	619	n_{69}	25.74	25.95	1706
n_{20}	32.85	54.51	506	n_{45}	45.62	24.59	619	n_{70}	29.09	23.02	0
n_{21}	44.68	48.65	2850	n_{46}	44.47	23.44	619	n_{71}	31.91	29.92	0
n_{22}	52.73	46.04	2297	n_{47}	46.25	22.18	0	n_{72}	20.30	44.26	0
n_{23}	43.84	45.10	1506	n_{48}	54.72	15.90	1246	n_{73}	77.32	16.74	0
n_{24}	44.05	43.53	1506	n_{49}	69.89	21.03	278	n_{74}	50.33	19.88	0
n_{25}	46.04	43.95	1506	n_{50}	76.80	7.22	963				

Table 1. Coordinates and population of nodes in the EMA highway benchmark network.

Edge	node pair	Edge	node pair	Edge	node pair
e_1	(n_1, n_3)	e_{44}	(n_{22}, n_{40})	e_{87}	(n_{44}, n_{46})
e_2	(n_1, n_7)	e_{45}	(n_{23}, n_{24})	e_{88}	(n_{44}, n_{54})
e_3	(n_1, n_9)	e_{46}	(n_{23}, n_{31})	e_{89}	(n_{45}, n_{46})
e_4	(n_2, n_3)	e_{47}	(n_{24}, n_{25})	e_{90}	(n_{45}, n_{47})
e_5	(n_3, n_6)	e_{48}	(n_{24}, n_{26})	e_{91}	(n_{46}, n_{47})
e_6	(n_3, n_7)	e_{49}	(n_{24}, n_{33})	e_{92}	(n_{46}, n_{54})
e_7	(n_4, n_6)	e_{50}	(n_{25}, n_{26})	e_{93}	(n_{47}, n_{48})
e_8	(n_4, n_8)	e_{51}	(n_{26}, n_{27})	e_{94}	(n_{47}, n_{74})
e_9	(n_5, n_{10})	e_{52}	(n_{26}, n_{28})	e_{95}	(n_{48}, n_{49})
e_{10}	(n_5, n_{11})	e_{53}	(n_{27}, n_{28})	e_{96}	(n_{48}, n_{51})
e_{11}	(n_6, n_8)	e_{54}	(n_{27}, n_{33})	e_{97}	(n_{48}, n_{52})
e_{12}	(n_6, n_{13})	e_{55}	(n_{27}, n_{35})	e_{98}	(n_{48}, n_{53})
e_{13}	(n_6, n_{17})	e_{56}	(n_{28}, n_{37})	e_{99}	(n_{48}, n_{54})
e_{14}	(n_7, n_9)	e_{57}	(n_{29}, n_{41})	e_{100}	(n_{48}, n_{74})
e_{15}	(n_7, n_{13})	e_{58}	(n_{29}, n_{49})	e_{101}	(n_{49}, n_{50})
e_{16}	(n_8, n_{11})	e_{59}	(n_{30}, n_{31})	e_{102}	(n_{49}, n_{73})
e_{17}	(n_8, n_{16})	e_{60}	(n_{30}, n_{60})	e_{103}	(n_{50}, n_{51})
e_{18}	(n_9, n_{12})	e_{61}	(n_{31}, n_{32})	e_{104}	(n_{50}, n_{73})
e_{19}	(n_9, n_{13})	e_{62}	(n_{31}, n_{60})	e_{105}	(n_{51}, n_{52})
e_{20}	(n_{10}, n_{11})	e_{63}	(n_{32}, n_{33})	e_{106}	(n_{52}, n_{53})
e_{21}	(n_{10}, n_{18})	e_{64}	(n_{32}, n_{34})	e_{107}	(n_{53}, n_{54})
e_{22}	(n_{10}, n_{20})	e_{65}	(n_{32}, n_{60})	e_{108}	(n_{55}, n_{57})
e_{23}	(n_{11}, n_{19})	e_{66}	(n_{33}, n_{34})	e_{109}	(n_{56}, n_{57})
e_{24}	(n_{13}, n_{14})	e_{67}	(n_{34}, n_{35})	e_{110}	(n_{57}, n_{58})
e_{25}	(n_{13}, n_{15})	e_{68}	(n_{34}, n_{60})	e_{111}	(n_{57}, n_{59})
e_{26}	(n_{14}, n_{17})	e_{69}	(n_{35}, n_{36})	e_{112}	(n_{58}, n_{59})
e_{27}	(n_{14}, n_{22})	e_{70}	(n_{35}, n_{71})	e_{113}	(n_{59}, n_{60})
e_{28}	(n_{16}, n_{17})	e_{71}	(n_{36}, n_{43})	e_{114}	(n_{59}, n_{72})
e_{29}	(n_{16}, n_{19})	e_{72}	(n_{36}, n_{44})	e_{115}	(n_{60}, n_{61})
e_{30}	(n_{16}, n_{22})	e_{73}	(n_{36}, n_{71})	e_{116}	(n_{60}, n_{63})
e_{31}	(n_{17}, n_{22})	e_{74}	(n_{37}, n_{38})	e_{117}	(n_{60}, n_{65})
e_{32}	(n_{18}, n_{19})	e_{75}	(n_{37}, n_{42})	e_{118}	(n_{60}, n_{67})
e_{33}	(n_{18}, n_{21})	e_{76}	(n_{38}, n_{39})	e_{119}	(n_{60}, n_{69})
e_{34}	(n_{19}, n_{22})	e_{77}	(n_{38}, n_{42})	e_{120}	(n_{60}, n_{71})
e_{35}	(n_{20}, n_{21})	e_{78}	(n_{39}, n_{40})	e_{121}	(n_{60}, n_{72})
e_{36}	(n_{20}, n_{30})	e_{79}	(n_{39}, n_{48})	e_{122}	(n_{62}, n_{63})
e_{37}	(n_{20}, n_{58})	e_{80}	(n_{40}, n_{41})	e_{123}	(n_{63}, n_{65})
e_{38}	(n_{21}, n_{22})	e_{81}	(n_{40}, n_{48})	e_{124}	(n_{64}, n_{65})
e_{39}	(n_{21}, n_{23})	e_{82}	(n_{41}, n_{49})	e_{125}	(n_{65}, n_{66})
e_{40}	(n_{22}, n_{23})	e_{83}	(n_{42}, n_{43})	e_{126}	(n_{67}, n_{68})
e_{41}	(n_{22}, n_{25})	e_{84}	(n_{42}, n_{45})	e_{127}	(n_{67}, n_{69})
e_{42}	(n_{22}, n_{28})	e_{85}	(n_{43}, n_{44})	e_{128}	(n_{69}, n_{70})
e_{43}	(n_{22}, n_{29})	e_{86}	(n_{43}, n_{45})	e_{129}	(n_{69}, n_{71})

Table 2. Edges (roadways) in the EMA highway benchmark network.

References

Markus Båth. Lateral inhomogeneities of the upper mantle. *Tectonophysics*, 2:483–514, 12 1965. ISSN 0040-1951. doi: 10.1016/0040-1951(65)90003-X.

Kenneth W. Campbell. Empirical near-source attenuation relationships for horizontal and vertical components of peak ground acceleration, peak ground velocity, and pseudo-absolute acceleration response spectra. *Seismological Research Letters*, 68:154–179, 1 1997. ISSN 0895-0695. doi: 10.1785/GSSRL.68.1.154.

P. Cosentino, V. Ficarra, and D. Luzio. Truncated exponential frequency-magnitude relationship in earthquake statistics. *Bulletin of the Seismological Society of America*, 67:1615–1623, 12 1977. ISSN 0037-1106. doi: 10.1785/BSSA0670061615.

K. R. Felzer and E. E. Brodsky. Decay of aftershock density with distance indicates triggering by dynamic stress. *Nature 2006 441:7094*, 441:735–738, 6 2006. ISSN 1476-4687. doi: 10.1038/nature04799.

Jayadipta Ghosh, Jamie E. Padgett, and Mauricio Sánchez-Silva. Seismic damage accumulation in highway bridges in earthquake-prone regions. *Earthquake Spectra*, 31:115–135, 2 2015. ISSN 19448201. doi: 10.1193/120812EQS347M;WEBSITE:WEBSITE:SAGE;WGROUP:STRING:PUBLICATION.

Y. J. Lee, J. Song, P. Gardoni, and H. W. Lim. Post-hazard flow capacity of bridge transportation network considering structural deterioration of bridges. *Structure and Infrastructure Engineering*, 7:509–521, 7 2011. ISSN 15732479. doi: 10.1080/15732479.2010.493338.

Paul A. Reasenberg and Lucile M. Jones. Earthquake hazard after a mainshock in california. *Science*, 243:1173–1176, 3 1989. ISSN 00368075. doi: 10.1126/SCIENCE.243.4895.1173;PAGE:STRING:ARTICLE/CHAPTER.

Tokuji Utsu, Yosihiko Ogata, Ritsuko S, and Matsu'ura. The centenary of the omori formula for a decay law of aftershock activity. *Journal of Physics of the Earth*, 43:1–33, 1995. ISSN 0022-3743. doi: 10.4294/JPE1952.43.1.